A coherent nonlinear optical signal induced by electron correlations

Shaul Mukamel[a)]
Department of Chemistry, University of California, Irvine, California 92697, USA

Rafał Oszwałdowski
Instytut Fizyki, Uniwersytet Mikołaja Kopernika, Grudziadzka 5/7, 87-100, Toruń, Poland and Department of Chemistry, University of California, Irvine, California 92697, USA

Lijun Yang
Department of Chemistry, University of California, Irvine, California 92697, USA

(Received 28 September 2007; accepted 9 November 2007; published online 13 December 2007)

The correlated behavior of electrons determines the structure and optical properties of molecules, semiconductors, and other systems. Valuable information on these correlations is provided by measuring the response to femtosecond laser pulses, which probe the very short time period during which the excited particles remain correlated. The interpretation of four-wave-mixing techniques, commonly used to study the energy levels and dynamics of many-electron systems, is complicated by many competing effects and overlapping resonances. Here we propose a coherent optical technique, specifically designed to provide a background-free probe for electronic correlations in many-electron systems. The proposed signal pulse is generated only when the electrons are correlated, which gives rise to an extraordinary sensitivity. The peak pattern in two-dimensional plots, obtained by displaying the signal versus two frequencies conjugated to two pulse delays, provides a direct visualization and specific signatures of the many-electron wave functions. © *2007 American Institute of Physics*. [DOI: 10.1063/1.2820379]

Predicting the energies and wave functions of interacting electrons lies at the heart of our understanding of all structural, optical, and transport properties of molecules and materials.[1–10] The Hartree–Fock (HF) approximation provides the simplest description of interacting fermions.[1,5] At this level of theory each electron moves in the average field created by the others. This provides a numerically tractable, uncorrelated-particle picture for the electrons, which approximates many systems well and provides a convenient basis for higher-level descriptions. Electronic dynamics is described in terms of orbitals, one electron at a time. Correlated n-electron wave functions, in contrast, live in a high $(3n)$ dimensional space and may not be readily visualized. Deviations from the uncorrelated picture (correlations) are responsible for many important effects. Correlation energies are comparable in magnitude to chemical bonding energies and are thus crucial for predicting molecular geometries and reaction barriers and rates with chemical accuracy. These energies can be computed for molecules by employing a broad arsenal of computational techniques such as perturbative corrections,[10] configuration interaction,[9] multideterminant techniques,[3] coupled cluster theory,[2] and time dependent density functional theory (TDDFT).[1,4,11] Correlation effects are essential in superconductors[7,8,12] and can be manipulated in artificial semiconductor nanostructures.[13–15] The fields of quantum computing and information are based on manipulating correlations between spatially separated systems, this is known as entanglement.[16]

In this article we propose a nonlinear optical signal that provides a unique probe for electron correlations. The technique uses a sequence of three optical pulses with wave vectors $\mathbf{k}_1$, $\mathbf{k}_2$, and $\mathbf{k}_3$, and detects the four wave mixing signal generated in the direction $\mathbf{k}_S=\mathbf{k}_1+\mathbf{k}_2-\mathbf{k}_3$ by mixing it with a fourth pulse (heterodyne detection).[17] We show that this correlation-induced signal, which depends parametrically on the consequent delays t_1, t_2, t_3 between pulses, vanishes for uncorrelated systems, providing a unique indicator of electron correlations. This technique opens up new avenues for probing correlation effects by coherent ultrafast spectroscopy.

Starting with the HF ground-state (g) of the system, each interaction with the laser fields can only move a single electron from an occupied to an unoccupied orbital. The first interaction generates a manifold (e) of single electron-hole (e-h) pair states. A second interaction can either bring the system back to the ground state or create a second e-h pair. We shall denote the manifold of doubly excited states as f (Fig. 1). We can go on to generate manifolds of higher levels. However, this will not be necessary for the present technique. The quantum pathways (i) and (ii) contributing to this signal can be represented by the Feynman diagrams[17] shown in Fig. 1. Each diagram shows the sequence of interactions of the system with the various fields and the state of the electron density matrix during each delay period. We shall display the signal as $S_{\mathrm{CI}}(\Omega_3,\Omega_2,t_1)$, where Ω_3 and Ω_2 are frequency variables conjugate to the delays t_3 and t_2 (Fig. 1) by a Fourier transform

[a)]Electronic mail: smukamel@uci.edu.

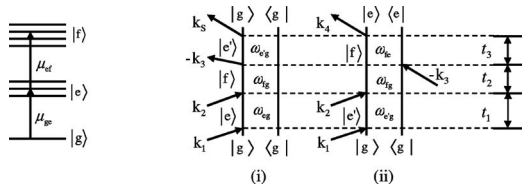

FIG. 1. Left: many-body states connected by transitions dipoles, including the ground state g, the manifold of single e-h pairs e, and the manifold of two-pair states f. Right: the two Feynman diagrams contributing to the correlation-induced signal S_{CI} [Eq. (1)]. t_i are the time delays between laser pulses. For independent electrons $\omega_{fe}=\omega_{e'g}$ and diagrams of types (i) and (ii) cancel in pairs.

$$S_{\mathrm{CI}}(\Omega_3,\Omega_2,t_1)=\int_0^\infty\int_0^\infty dt_2dt_3S_{\mathrm{CI}}(t_3,t_2,t_1)\times\exp(i\Omega_2t_2+i\Omega_3t_3),$$

with t_1 fixed. This yields an expression for the exact response function

$$S_{\mathrm{CI}}(\Omega_3,\Omega_2,t_1=0)=\sum_{e,e',f}\frac{1}{\Omega_2-\omega_{fg}}\left[\frac{\mu_{ge}\mu_{ef}\mu_{fe'}\mu_{e'g}}{\Omega_3-\omega_{e'g}}-\frac{\mu_{ge'}\mu_{e'f}\mu_{fe}\mu_{eg}}{\Omega_3-\omega_{fe}}\right],\quad(1)$$

where for simplicity we set $t_1=0$. Two-dimensional correlation plots of Ω_2 versus Ω_3 then reveal a characteristic peak pattern, which spans the spectral region permitted by the pulse bandwidths. The two terms in the brackets correspond respectively to diagrams (i) and (ii) of Fig. 1. Here $\mu_{\nu\nu'}$ are the transition dipoles and $\omega_{\nu\nu'}$ are the transition energies between electronic states, shifted by the pulse carrier frequency ω_0, i.e., $\omega_{e'g}=\epsilon_{e'}-\epsilon_g-\omega_0$, $\omega_{fe}=\epsilon_f-\epsilon_e-\omega_0$, and $\omega_{fg}=\epsilon_f-\epsilon_g-2\omega_0$. This shift eliminates the high optical frequencies. The carrier frequency of the three beams, ω_0, is held fixed and used to select the desired spectral region. In Eq. (1) we have invoked the rotating wave approximation and only retained the dominant terms where all fields are resonant with an electronic transition.

In both diagrams, during t_2 the system is in a coherent superposition (coherence) between the doubly excited state f and the ground state g. This gives the common prefactor $(\Omega_2-\omega_{fg})^{-1}$. As Ω_2 is scanned, the signal will thus show resonances corresponding to the different doubly excited states f. However, the projection along the other axis (Ω_3) is different for the two diagrams. In diagram (i), the system is in a coherence between e' and g during t_3. As Ω_3 is scanned, the first term in brackets reveals single excitation resonances when $\Omega_3=\omega_{e'g}$. For the second diagram (ii), the system is in a coherence between f and e during t_3. This gives resonances at $\Omega_3=\omega_{fe}$ in the second term in the brackets. Many new peaks corresponding to all possible transitions between doubly and singly excited states ω_{fe} should then show up.

The remarkable point that makes this technique so powerful is that the two terms in Eq. (1) interfere in a very special way. For independent electrons, where correlations are totally absent, the two e-h pair state f is simply given by a direct product of the single pair states e and e', and the double-excitation energy is the sum of the single-excitation energies $\epsilon_f=\epsilon_e+\epsilon_{e'}$, so that $\omega_{e'g}=\omega_{fe}$ and the two terms in the brackets exactly cancel. The density functional theory,[1,4,11] when implemented using the Kohn–Sham approach, gives a set of orbitals that carry some information about correlations in the ground state. The signal calculated using transitions between Kohn–Sham orbitals will vanish as well. This will be the case for any uncorrelated-particle calculation that uses transitions between fixed orbitals, no matter how sophisticated the procedure was used to compute these orbitals. We expect the resonance pattern of the two-dimensional S_{CI} signal to provide a characteristic fingerprint for electron correlations.

The following simulations carried out for simple model systems, which contain a few orbitals and electrons, illustrate the power of the proposed technique. Doubly excited states can be expressed as superpositions of products of two e-h pair states. Along Ω_2 we should see the various doubly excited states at ω_{fg}, whereas along Ω_3 we observe the various projections of the f state onto single pair states $\omega_{e'g}$ and the differences $\omega_{fe}=\omega_{fg}-\omega_{eg}$. The two-dimensional (2D) spectra thus provide direct information about the nature of the many body wave functions that is very difficult to measure by other means. The patterns predicted by different levels of electronic structure simulations provide a direct means for comparing their accuracy. We used a tight-binding Hamiltonian $H=H_0+H_C+H_L$. The single-particle contribution H_0 contains orbital energies and hoppings

$$H_0=\sum_{m_1,n_1}t_{m_1,n_1}c^\dagger_{m_1}c_{n_1}+\sum_{m_2,n_2}t_{m_2,n_2}d^\dagger_{m_2}d_{n_2},$$

where c_{n_1} and d_{n_2} are electron and hole annihilation operators, respectively, and the summations run over spin orbitals. We assume equal hopping t for electrons and holes. The many-body term responsible for correlations

$$H_C=\frac{1}{2}\sum_{m_1,n_1}V^{\mathrm{ee}}_{m_1n_1}c^\dagger_{m_1}c^\dagger_{n_1}c_{n_1}c_{m_1}+\frac{1}{2}\sum_{m_2,n_2}V^{\mathrm{hh}}_{m_2n_2}d^\dagger_{m_2}d^\dagger_{n_2}d_{n_2}d_{m_2}-\sum_{m_1,m_2}V^{\mathrm{eh}}_{m_1m_2}c^\dagger_{m_1}d^\dagger_{m_2}d_{m_2}c_{m_1}$$

contains only direct Coulomb couplings. The electron-electron, hole-hole, and electron-hole interactions are denoted V^{ee}, V^{hh}, and V^{eh}, respectively. Values of t and the Coulomb integrals V^{eh}_{00}, V^{eh}_{01} (subscripts 0 and 1 denote the sites) were derived by fitting emission spectra of coupled quantum dots.[18] Owing to the nature of quantum dots states, we can assume that $V^{\mathrm{eh}}\simeq V^{\mathrm{ee}}\simeq V^{\mathrm{hh}}$.[19] We choose $V^{\mathrm{ee}}=V^{\mathrm{hh}}=1.2V^{\mathrm{eh}}$ and use these values for all orbitals. H_L describes the dipole interaction with the laser pulses, $H_L=-E(t)\mu_{m_1m_2}d_{m_2}c_{m_1}+h\cdot c$, where $E(t)$ is the light field and $\mu_{m_1m_2}$ are local dipole moments of various orbitals m_1, m_2. ω_0 was tuned to the optical gap energy.

Even though our parameters are fitted to quantum dots, the overall picture emerging from the calculations can be applied to a wider class of systems, whose optical response is determined by correlated e-h pairs. We have employed an equation of motion approach for computing the signal.

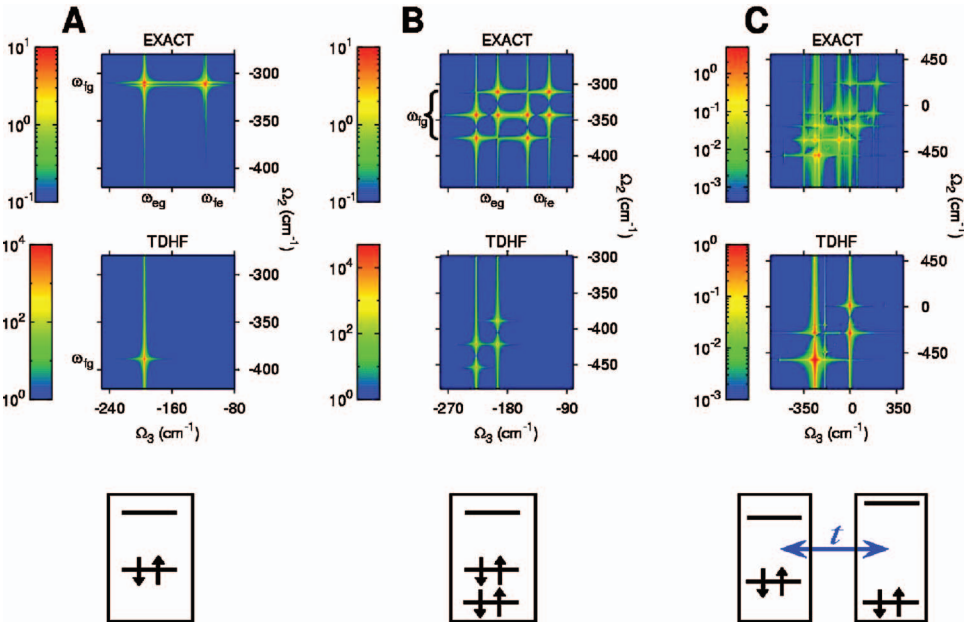

FIG. 2. (Color) Absolute value of the exact and the TDHF S_{CI} signals for three model systems. Energies on the axes are referenced to the carrier frequency, which excites interband transitions. Each system has $N(N+1)/2$ doubly excited levels, where N is the number of single-excited levels. (A) Two orbital system with $N=1$($V^{\mathrm{eh}}=194.4$ cm^{-1}), (B) three orbital system with $N=2$($V^{\mathrm{eh}}=194.4$ cm^{-1}), (C) two coupled systems of type (a), but with different gaps, $V^{\mathrm{eh}}=193.9$ cm^{-1} for one dot and 78.1 cm^{-1} for the other and $t=59.2$ cm^{-1}, $N=4$. The corresponding orbitals and splittings are given schematically below each panel. For systems (A) and (B), the TDHF misses half of the resonances along Ω_3, while for (C) it misses four out of ten resonances along Ω_2.

Many-body states are never calculated explicitly in this algorithm. Instead, we obtain the signal directly by solving the nonlinear exciton equations (NEE).[20,21] These equations describe the coupled dynamics of two types of variables representing single e-h pairs: $B_m=\langle d_{m_2}c_{m_1}\rangle$ [here $m=(m_1,m_2)$ stands for both the electron index m_1 and the hole index m_2] and two pairs $Y_{mn}=\langle d_{m_2}c_{m_1}d_{n_2}c_{n_1}\rangle$. For our model the NEE is equivalent to full CI and yield the exact signal with all correlation effects fully included. This signal provides a direct experimental test for many-body theories, which use various degrees of approximations to treat electron correlations. We compare the exact calculation (NEE) with the time dependent Hartree–Fock (TDHF) theory, which is an approximate, widely used technique for treating correlations by factorizing the Y variables into $\langle d_{m_2}c_{m_1}\rangle\langle d_{n_2}c_{n_1}\rangle-\langle d_{n_2}c_{m_1}\rangle\langle d_{m_2}c_{n_1}\rangle$. This assumes that two e-h pairs are independent and we only need to solve the equations for $\langle d_{n_2}c_{n_1}\rangle$. Correlation within e-h pairs is nevertheless retained by this level of theory, as evidenced by the finite S_{CI} signal. The equations of motion derived using both levels of factorization are solved analytically, yielding the exact and the TDHF S_{CI} signals. The TDHF solutions have the following structure: A set of single-particle excitations with energies ϵ_α and the corresponding transition dipole moments are obtained by solving the linearized TDHF equations. Many-particle state energies are given by sums of these elementary energies. Two-particle energies are of the form $\epsilon_\alpha+\epsilon_\beta$. This approximation is the price we pay for the enormous simplicity and convenience of TDHF. Correlated many-electron energies computed by higher level techniques do not possess this additivity property.

In general the TDHF signal contains a different number of resonances along Ω_2 than the exact one. Their positions, $\omega_{fg}=\epsilon_f-\epsilon_g$, also differ since the former uses the additive approximation for the energies ϵ_f. The Ω_3 value of each resonance in the exact simulation is given by either $\omega_{e'g}$ [first term in brackets in Eq. (1)] or ω_{fe} (second term in brackets). The simulations of the TDHF response function presented later show fewer peaks than in the exact calculation. This dramatic effect reflects direct signatures of the correlated two e-h pair wave functions, which are only revealed by the S_{CI} technique.

We first consider a simple model, consisting of a single site with one valence orbital and one conduction orbital [Fig. 2(A)]. The energy of the (spin-degenerate) single-pair state is $\epsilon_e=-V^{\mathrm{eh}}$. The only two-pair state has energy $\epsilon_f=-4V^{\mathrm{eh}}+V^{\mathrm{ee}}+V^{\mathrm{hh}}$, compared with $\bar{\epsilon}_f=2\epsilon_e$ in the TDHF approximation (the TDHF double-excited energies and frequencies will be marked with a bar: $\bar{\epsilon}_f$, $\bar{\omega}_{fe}$). Thus, the exact signal has two peaks at $(\Omega_3,\Omega_2)=(\omega_{eg},\omega_{fg})$ and $(\omega_{fe},\omega_{fg})$, while TDHF predicts only one peak at $(\Omega_3,\Omega_2)=(\omega_{eg},\bar{\omega}_{fg})=(\bar{\omega}_{fe},\bar{\omega}_{fg})$.

This high sensitivity to correlation effects is general and is maintained in more complex systems. In Fig. 2(B) we consider a system with two valence orbitals with a splitting Δ and one conduction orbital. It has two single e-h pair transitions e_1, e_2 with energies $\epsilon_1=-V^{\mathrm{eh}}$ and $\epsilon_2=-V^{\mathrm{eh}}+\Delta$. The exact spectrum contains eight peaks, with ϵ_f energies being sums of all quasiparticle interactions and hole level energies: $\epsilon_{f_1}=-4V^{\mathrm{eh}}+V^{\mathrm{ee}}+V^{\mathrm{hh}}$, $\epsilon_{f_2}=\epsilon_{f_1}+\Delta$, $\epsilon_{f_3}=\epsilon_{f_1}+2\Delta$. Within TDHF we find $\bar{\epsilon}_{f1}=2\epsilon_1$, $\bar{\epsilon}_{f_2}=\epsilon_1+\epsilon_2$, and $\bar{\epsilon}_{f_3}=2\epsilon_2$ and the 2D spectrum only shows four peaks.

The simple energy-level structure of the two systems [Figs. 2(A) and 2(B)], whereby $\bar{\omega}_{fe}=\omega_{eg}$, allows an insight into the differences in predictions of the two response functions. We recast Eq. (1) for the exact signal in a slightly different form: $(\Omega_2-\omega_{fg})^{-1}(\Omega_3-\omega_{e'g})^{-1}(\Omega_3-\omega_{fe})^{-1}$ (all dipoles for this system are equal $\mu_{ge'}=\mu_{ge}=\mu_{e'f}$, etc.).

The corresponding TDHF expression is: $(\Omega_2-\bar{\omega}_{fg})^{-1}(\Omega_3-\omega_{e'g})^{-2}$. The different Ω_3 dependencies reflect different numbers of resonances with different full width at half maximum along the Ω_3 axis. The double resonance in TDHF is split into two resonances in the exact expression.

Figure 2(C) shows the signal from two coupled quantum dots, each hosting one valence and one conduction orbital. The S_{CI} signal contains a rich peak structure, reflecting the four (ten) many body levels in the single- (double-) excited manifold. Again, the TDHF method misses many peaks. In this case, unlike the two previous systems, TDHF does not show all possible resonances along the Ω_2 axis. This is because one of the single-excited states (e_1) is not optically allowed. In TDHF any f state, constructed as a direct product of e_1 with another state e_i $(i=1,\ldots,4)$, is forbidden. Thus we have only six resonances. In the exact calculation, the f states are not direct products, so we see all possible resonances along Ω_2. The differences between the TDHF and exact spectra in all these examples illustrate the sensitivity of the proposed signal to the correlated wave function.

Computing electron correlation effects, which are neglected by HF theory, constitutes a formidable challenge of many-body theory. Each higher-level theory for electron correlations[1,4] is expected to predict a distinct two-dimensional signal, which will reflect the accuracy of its energies and many-body wave functions. The proposed technique thus offers a direct experimental test for the accuracy of the energies as well as the many-body wave functions calculated by different approaches. TDDFT within the adiabatic approximation extends TDHF to better include exchange and correlation effects.[4,11] However, the two are formally equivalent and yield a similar excited-state structure.[22] The two-dimensional peak pattern of TDDFT will suffer from the same limitations of TDHF.

We can summarize our findings as follows: At the HF level which assumes independent electrons, the S_{CI} signal vanishes due to interference. TDHF (or TDDFT) goes one step further and provides a picture of independent transitions (quasiparticles). Here the signal no longer vanishes but shows a limited number of peaks. When correlation effects are fully incorporated, the many-electron wave functions become superpositions of states with different numbers and types of e-h pairs. The Ω_2 and Ω_3 axes will then contain many more peaks corresponding to all many body states (in the frequency range spanned by the pulse bandwidths), which project into the doubly excited states. Thus, along Ω_2 the peaks will be shifted, reflecting the level of theory used to describe electron correlations. Along Ω_3, the effect is even more dramatic and new peaks will show up corresponding to splittings between various levels. This highly resolved two-dimensional spectrum provides an invaluable direct dynamical probe of electron correlations (both energies and wave functions).

Signals obtained from a similar pulse sequence, calculated for electronic transitions in molecular aggregates[23] and molecular vibrations,[24] show the role of coupling between Frenkel excitons. A conceptually related nuclear magnetic resonance technique known as double quantum coherence reveals correlation effects among spins. The technique showed unusual sensitivity for weak couplings between spatially remote spins and has been used to develop new magnetic resonance imaging techniques.[25,26] Here we have extended this idea to all many-electron systems. The proposed technique should apply to molecules, atoms, quantum dots, and highly correlated systems such as superconductors. It has been recently demonstrated that two-exciton couplings can be controlled in onionlike semiconductor nanoparticles with a core and an outer shell made of different materials.[13] Nonlinear spectroscopy of the kind proposed here could provide invaluable insights into the nature of such two-exciton states.

This research was supported by the National Science Foundation Grant No. CHE-0446555 and the National Institute of Health Grant No. GM59230.

[1] G. F. Giuliani and G. Vignale, *Quantum Theory of the Electron Liquid* (Cambridge University Press, Cambridge, 2005).
[2] R. J. Bartlett and M. Musial, Rev. Mod. Phys. **79**, 291 (2007).
[3] B. Roos, Acc. Chem. Res. **32**, 137 (1999).
[4] *Time-Dependent Density Functional Theory*, edited by M. A. L. Marques, C. A. Ullrich, F. Nogueira, A. Rubio, K. Burke, and E. K. U. Gross (Springer, Berlin, 2006).
[5] P. Fulde, *Electron Correlations in Molecules and Solids*, 3rd ed. (Springer, Berlin, 1984).
[6] *Recent Advances in Electron Correlation Methodology*, ACS Symposium Series, edited by A. K. Wilson and K. A. Peterson (American Chemical Society, Washington, DC, 2007).
[7] P. A. Lee, N. Nagaosa, and X.-G. Wen, Rev. Mod. Phys. **78**, 17 (2006).
[8] G. Kotliar, S. Y. Savrasov, K. Haule, V. S. Oudovenko, O. Parcollet, and C. A. Marianetti, Rev. Mod. Phys. **78**, 865 (2006).
[9] C. D. Sherrill and H. F. Schaefer, *Advances in Quantum Chemistry* (Academic, New York, 1999), Vol. 34.
[10] L. A. Curtiss, K. Raghavachari, P. C. Redfern, V. Rassolov, and J. A. Pople, J. Chem. Phys. **109**, 7764 (1998).
[11] G. Onida, L. Reining, and A. Rubio, Rev. Mod. Phys. **74**, 601 (2002).
[12] R. A. Kaindl, M. Woerner, T. Elsaesser, D. C. Smith, J. F. Ryan, G. A. Farnan, M. P. McCurry, and D. G. Walmsley, Science **287**, 470 (2000).
[13] V. I. Klimov, S. A. Ivanov, J. Nanda, M. Achermann, I. Bezel, J. A. McGuire, and A. Piryatinski, Nature (London) **447**, 441 (2007).
[14] F. Rossi and T. Kuhn, Rev. Mod. Phys. **74**, 895 (2002).
[15] D. S. Chemla and J. Shah, Nature (London) **411**, 549 (2001).
[16] M. A. Nielsen and L. I. Chuang, *Quantum Computation and Quantum Information* (Cambridge University Press, Cambridge, 2000).
[17] S. Mukamel, *Principles of Nonlinear Optical Spectroscopy* (Oxford University Press, New York, 1995).
[18] M. Bayer, P. Hawrylak, K. Hinzer, S. Fafard, M. Korkusinski, Z. R. Wasilewski, O. Stern, and A. Forchel, Science **291**, 451 (2001).
[19] M. Bayer, O. Stern, P. Hawrylak, S. Fafard, and A. Forchel, Nature (London) **405**, 923 (2000).
[20] V. Chernyak, W. M. Zhang, and S. Mukamel, J. Chem. Phys. **109**, 9587 (1998).
[21] V. M. Axt and S. Mukamel, Rev. Mod. Phys. **70**, 145 (1998).
[22] O. Berman and S. Mukamel, Phys. Rev. A **67**, 042503 (2003).
[23] S. Mukamel, Annu. Rev. Phys. Chem. **51**, 691 (2000).
[24] W. Zhuang, D. Abramavicius, and S. Mukamel, Proc. Natl. Acad. Sci. U.S.A. **102**, 7443 (2005).
[25] W. Richter and W. S. Warren, Concepts Magn. Reson. **12**, 396 (2000).
[26] S. Mukamel and A. Tortschanof, Chem. Phys. Lett. **357**, 327 (2002).